Inorg. Chem. **1995**, *34*, 6514−6519

Synthesis, Structural Characterization, and Spectroscopic Studies of Heterodimetallic $[NBu_4][(C_6F_5)_3Pt(\mu\text{-}Pb)(\mu\text{-}X)Pt(C_6F_5)_3]$ (X = Cl, OH) Complexes

José María Casas,[†] Juan Forniés,*[,†] Antonio Martín,[‡] Víctor M. Orera,[§] A. Guy Orpen,[‡] and Angel J. Rueda[†]

Departamento de Química Inorgánica and Instituto de Ciencia de Materiales de Aragón, Universidad de Zaragoza—CSIC, 50009 Zaragoza, Spain, and School of Chemistry, University of Bristol, Bristol, U.K. BS8 1TS

Received July 7, 1995[®]

Anionic heterobinuclear complexes with molecular formula $[NBu_4][(C_6F_5)_3Pt(\mu\text{-}Pb)(\mu\text{-}X)Pt(C_6F_5)_3]$ (X = Cl (**1**), I (**2**), OH (**3**)) were obtained by the reaction of $[NBu_4]_2[Pt(C_6F_5)_3X]$ (X = Cl, I) and $Pb(ClO_4)_2{\cdot}3H_2O$ in CH_2Cl_2 or alternatively by substitution of the Cl by the OH group in the trinuclear final product. Structures of complexes **1** and **3** were determined by single crystal X-ray diffraction, confirming the presence of two Pt−Pb bonds in each case. The Pb centers also display *o*-F···Pb short nonbonding contacts which can also be observed in solution. Compound **1** ($C_{52}H_{36}ClF_{30}NPbPt_2$) crystallizes in the monoclinic system, space group *C*2/*c*: $a = 32.121(6)$ Å, $b = 17.828(4)$ Å, $c = 19.389(5)$ Å, $\beta = 93.37(3)°$, $V = 11084(4)$ Å^3, $Z = 8$. The bond distances between the metal atoms are Pt(1)−Pb = 2.721(1) Å and Pt(2)−Pb = 2.729(1) Å. Compound **3** ($C_{52}H_{37}F_{30}NOPbPt_2$) crystallizes in the triclinic system, space group $P\bar{1}$: $a = 10.707(4)$ Å, $b = 15.863(6)$ Å, $c = 17.828(5)$ Å, $\alpha = 104.57(3)°$, $\beta = 98.97(3)°$, $\gamma = 100.05(3)°$, $V = 2822(2)$ Å^3, $Z = 2$. The bond distances between the metal atoms are Pt(1)−Pb = 2.701(1) Å and Pt(2)−Pb = 2.712(1) Å.

Introduction

It is now well-established that anionic perhalophenyl platinate complexes behave as Lewis bases and react with metal (M) complexes or metal salts, yielding polynuclear species with donor−acceptor Pt → M bonds.[1] Most of these complexes are formed by reaction of the platinate substrates with silver derivatives, although recently complexes with Pt → Hg,[2] Pt → Pb,[3] or Pt → Tl[4] bonds have also been described. The nature of the resulting complexes is strongly dependent on the type of platinate substrates used as starting materials.

Recently, the synthesis and structural characterization of the trinuclear compound $[NBu_4]_2[Pb\{Pt(C_6F_5)_4\}_2]$,[3] which contains lead linearly bonded to two platinum centers, has been described. The stability of this compound, which is formed by reaction of $[NBu_4]_2[Pt(C_6F_5)_4]$ and $Pb(NO_3)_2$ in MeOH, is mainly due to the Pt → Pb donor−acceptor interactions between the platinate(II) moieties and Pb^{2+}.

Recently, special attention has been paid to these heterobimetallic complexes, which contain at least one transition metal center, because of their spectroscopic and particularly their luminescent properties.[5−9]

In this paper we report a study of the reactions of $[NBu_4]$-$[Pt(C_6F_5)_3X]$ (X = Cl, I) with $Pb(ClO_4)_2$ which takes place with PbX_2 elimination and formation of the trinuclear compounds $[NBu_4]_2[(C_6F_5)_3Pt(\mu\text{-}Pb)(\mu\text{-}X)Pt(C_6F_5)_3]$, which contain lead bonded to two platinum centers in a bent arrangement.

Experimental Section

General Procedures. C, H, and N analyses were performed with a Perkin-Elmer 240B microanalyzer. The IR spectra were recorded over the range 200−4000 cm^{-1} on a Perkin-Elmer 883 spectrophotometer from Nujol mulls between polyethylene sheets. The ^{1}H and ^{19}F NMR spectra were obtained on a Brüker ARX 300 or on a Varian Unity 300 instrument in $CDCl_3$ solutions. Negative ion FAB mass spectra were recorded on a VG-Autospec spectrometer operating at ca. 30 kV, using the standard cesium FAB gun and 3-nitrobenzyl alcohol (3-NOBA) as matrix. Literature methods were used to prepare the starting $[NBu_4]_2[Pt(C_6F_5)_3X]$ (X = Cl, I) compounds.[10]

Preparation of $[NBu_4][(C_6F_5)_3Pt(\mu\text{-}Pb)(\mu\text{-}Cl)Pt(C_6F_5)_3]$ (1). To a solution of $[NBu_4]_2[Pt(C_6F_5)_3Cl]$ (0.200 g, 0.164 mmol) in 30 mL of CH_2Cl_2 was added an equimolar amount of $Pb(ClO_4)_2{\cdot}3H_2O$ (0.076 g, 0.164 mmol), and the mixture was stirred at room temperature for 3 h. The unreacted $Pb(ClO_4)_2$ and the $PbCl_2$ precipitated were filtered off, and the resulting solution was evaporated to dryness; after evaporation the residue was treated with 20 mL of ^{i}PrOH, giving rise to complex **1** as a yellow solid (70% yield). Anal. Found (Calcd): C, 33.05 (33.26); H, 1.77 (1.93); N, 0.71 (0.74). IR (cm^{-1}): C_6F_5, 1639 s, 1612 m, 1511 vs, 1504 vs, 1348 s, 1060 vs, 962 vs; X-sensitive mode,[11] 809 vs, 794 s, 781 vs; ν(Pt−Cl), 292 m. FAB$^-$ MS: *m*/*z* 1635 $[Pt_2Pb(C_6F_5)_6Cl]^-$. ^{19}F NMR ($CDCl_3$): δ −117.9 [m$_c$, $^3J(^{195}Pt,F) = 331$ Hz, 2F, *o*-F], −119.1 [m$_c$, $^3J(^{195}Pt,F) = 190$ Hz, 4F, *o*-F], −119.4 [m$_c$, $^3J(^{195}Pt,F) = 187$ Hz, 4F, *o*-F], −130.8 (m$_c$, $^3J(^{195}Pt,F) = 259$ Hz, 2F, *o*-F], −159.5 (t, 4F, *p*-F), −160.6 (t, 2F, *p*-F), −161.5 (m$_c$, 4F, *m*-F), −162.3 (m$_c$, 2F, *m*-F), −162.5 (m$_c$, 4F, *m*-F), −162.9 (m$_c$, 2F, *m*-F).

[†] Departamento de Química Inorgánica, Universidad de Zaragoza.

[‡] University of Bristol.

[§] Instituto de Ciencia de Materiales de Aragón, Universidad de Zaragoza.

[®] Abstract published in *Advance ACS Abstracts*, November 15, 1995.

(1) Usón, R.; Forniés, J. *Inorg. Chim. Acta.* **1992**, *198−200*, 165, and references cited therein.

(2) Usón, R.; Forniés, J.; Falvello, L. R.; Ara, I.; Usón, I. *Inorg. Chim. Acta* **1993**, *212*, 105.

(3) Usón, R.; Forniés, J.; Falvello, L. R.; Usón, M. A.; Usón, I. *Inorg. Chem.* **1992**, *31*, 3697.

(4) Usón, R.; Forniés, J.; Tomás, M.; Garde, R.; Alonso, P. J. *J. Am. Chem. Soc.* **1995**, *117*, 1837.

(5) Wang, S.; Garzón, G.; King, C.; Wang, J.-C.; Fackler, J. P., Jr. *Inorg. Chem.* **1989**, *28*, 4623.

(6) Balch, A. L.; Catalano, V. J.; Chatfield, M. A.; Nagle, J. K.; Olmstead, M. M.; Reedy, P. E., Jr. *J. Am. Chem. Soc.* **1991**, *113*, 1252.

(7) Yip, H.-K.; Lin, H.-M.; Wang, Y.; Che, Ch.-M. *Inorg. Chem.* **1993**, *32*, 3402.

(8) Yip, H.-K.; Cheng, L.-K.; Wang, Y.; Cheung, K.-K.; Che, Ch.-M. *J. Chem. Soc., Dalton Trans.* **1993**, 2933.

(9) Yip, H.-K.; Lin, H.-M.; Wang, Y.; Che, Ch.-M. *J. Chem. Soc., Dalton Trans.* **1993**, 2939.

(10) Usón, R.; Forniés, J.; Tomás, M.; Fandos, R. *J. Organomet. Chem.* **1984**, *263*, 253.

0020-1669/95/1334-6514$09.00/0

Table 1. Crystal Data and Structure Refinement for **1** and **3**[a]

	1	**3**
empirical formula	$C_{52}H_{36}ClF_{30}NPbPt_2$	$C_{52}H_{37}F_{30}NOPbPt_2$
fw	1877.64	1859.20
temp	173(2) K	293(2) K
wavelength, Å	0.710 73	0.710 73
cryst syst	monoclinic	triclinic
space group	C2/c	$P\bar{1}$
a, Å	32.121(6)	10.707(4)
b, Å	17.828(4)	15.863(6)
c, Å	19.389(4)	17.828(5)
α, deg	90	104.57(3)
β, deg	93.37(3)	98.97(3)
γ, deg	90	100.05(3)
V, Å^3	11084(4)	2822(2)
Z	8	2
cryst size, mm	0.50 × 0.50 × 0.45	0.40 × 0.25 × 0.25
D_{calc}, Mg/m^3	2.250	2.188
absorpn coeff, mm^{-1}	8.254	8.061
scan range	$2.5 < 2\theta < 46.6$	$3 < 2\theta < 50$
reflecns collected	17 897	10 532
independ reflecns	7971 [$R_{int} = 0.0656$]	9950 [$R_{int} = 0.0652$]
data/restraints/parameters	7961/0/794	9947/2/709
goodness-of-fit on F^2, S	1.392	1.024
final *R* indices [$I > 2\sigma(I)$]	$R_1 = 0.0455$, $R_{2w} = 0.1094$	$R_1 = 0.0618$, $R_{2w} = 0.0851$
R indices (all data)	$R_1 = 0.0606$, $R_{2w} = 0.1213$	$R_1 = 0.1535$, $R_{2w} = 0.1277$
largest diff peak and hole, e$^-$ Å^{-3}	1.52/−1.59	0.82/−0.74

[a] $R_1 = \sum|F_o - F_c|/\sum|F_o|$; $R_{2w} = [\sum[w(F_o^2 - F_c^2)^2/\sum[w(F_o^2)^2]^{1/2}$; $S = [\sum w(F_o^2 - F_c^2)^2/((\text{no ref}) - (\text{no par}))]^{1/2}$; no ref = number of reflections; no par = number of parameters.

Preparation of $[NBu_4][(C_6F_5)_3Pt(\mu\text{-}Pb)(\mu\text{-}I)Pt(C_6F_5)_3]$ (2). To a solution of $[NBu_4]_2[Pt(C_6F_5)_3I\}$ (0.288 g, 0.220 mmol) in 30 mL of CH_2Cl_2 was added $Pb(ClO_4)_2{\cdot}3H_2O$ (0.060 g, 0.1126 mmol, 15% excess), and the mixture was stirred at room temperature for 3 h. The unreacted $Pb(ClO_4)_2$ and the PbI_2 formed were filtered off. The resulting solution was evaporated to dryness, and the residue was treated with 5 mL of ^iPrOH and 40 mL of H_2O, rendering complex **2** as a yellow solid (70% yield). Anal. Found (Calcd): C, 32.12 (31.72); H, 1.75 (1.84); N, 0.90 (0.71). IR (cm^{-1}): C_6F_5, 1640 s, 1610 m, 1502 vs, 1347 vs, 1056 vs, 963 vs; X-sensitive mode,[11] 804 vs, 791 s, 780 vs. FAB$^-$ MS: *m/z* 1727 $[Pt_2Pb(C_6F_5)_6I]^-$. ^{19}F NMR ($CDCl_3$): δ −114.7 (m$_c$, 4F, *o*-F), −119.0 (m$_c$, 6F, *o*-F), −126.5 (m$_c$, 2F, *o*-F), −160.2 (t, 4F, *p*-F), −160.7 (t, 2F, *p*-F), −162.1 (m$_c$, 4F, *m*-F), −162.5 (m$_c$, 8F, *m*-F).

Preparation of $[NBu_4][(C_6F_5)_3Pt(\mu\text{-}Pb)(\mu\text{-}OH)Pt(C_6F_5)_3]$ (3). (A) To a solution of $[NBu_4\}_2[Pt(C_6F_5)_3Cl]$ (0.200 g, 0.164 mmol) in 30 mL of CH_2Cl_2, 0.10 mL (0.082 mmol) of NBu_4OH/MeOH (0.8 M) was added, and, after 5 min of stirring at room temperature, 0.076 g (0.164 mmol) of $Pb(ClO_4)_2{\cdot}3H_2O$ were added to the resulting solution. After 4 h of stirring the unreacted $Pb(ClO_4)_2$, which remained in suspension, and the $PbCl_2$ precipitated were filtered off, and the resulting solution was evaporated to dryness. The residue was treated with 30 mL of Et_2O, giving NBu_4ClO_4, which was separated by filtration. The diethyl ether solution was evaporated to dryness, and 20 mL of *n*-hexane was added to the residue, rendering complex **3** as a yellow solid (73% yield). Anal. Found (Calcd): C, 34.10 (33.60); H, 2.10 (2.01); N, 0.91 (0.75). IR (cm^{-1}): C_6F_5, 1637 m, 1609 m, 1509 vs, 1347 s, 1062 vs, 962 vs; X-sensitive mode,[11] 808 vs, 795 s, 782 vs; ν(O−H), 3609 m. FAB$^-$ MS: *m/z* 1616 $[Pt_2Pb(C_6F_5)_6(OH)]^-$. ^{19}F NMR ($CDCl_3$): δ −121.6 [m$_c$, $^3J(^{195}Pt,F) = 317$ Hz, 2F, *o*-F), −122.8 (m$_c$, 4F, *o*-F), −123.5 (m$_c$, 4F, *o*-F), −134.4 [m$_c$, $^3J(^{195}Pt,F) = 254$ Hz, 2F, *o*-F], −163.1 (t, 4F, *p*-F), −164.3 (t, 2F, *p*-F), −165.5 (m$_c$, 4F, *m*-F), −165.5 (m$_c$, 2F, *m*-F), −165.8 (m$_c$, 4F, *m*-F), −166.5 (m$_c$, 2F, *m*-F).

(B) A CH_2Cl_2 (20 mL) solution of 0.1 g (0.053 mmol) of **1** was stirred with 0.1 mL of H_2O for 48 h. The solution was evaporated to dryness and the residue treated with 20 mL of *n*-hexane, giving complex **3** as a yellow precipitated (87% yield).

Preparation of Crystals for X-ray Structure Determination. Suitable crystals of **1** (X = Cl) and **3** (X = OH) for X-ray purposes were obtained by slow diffusion of *n*-hexane into a solution of 0.03 g of $[NBu_4][C_6F_5)_3Pt(\mu\text{-}Pb)(\mu\text{-}X)Pt(C_6F_5)_3]$ in CH_2Cl_2 (4 mL) at −30 °C.

X-ray Structure Analysis of 1. A crystal of **1** (approximate dimensions 0.50 × 0.50 × 0.45 mm) was glued with epoxy adhesive to the end of a glass fiber. All diffraction measurements were made at 173 K on a Siemens three-circle SMART[12] area detector diffractometer using graphite monochromated Mo Kα radiation. Table 1 summarizes the crystallographic data, details associated with data collection, and least squares residuals for the crystal determination of **1**. Crystal quality was assessed and unit cell dimensions were determined from 263 reflections taken from 3 sets of 30 frames (at 0.3-deg steps in ω). A full hemisphere of reciprocal space was scanned by 0.3-deg ω steps and 10 s exposures with the area detector center held at $2\theta = -23°$. A total of 17 897 reflection intensities were integrated to $d_{min} = 0.90$ Å using the SAINT[13] program. An absorption correction was applied on the basis of 16 810 symmetry equivalent data (maximum and minimum transmission coefficients were 0.975 and 0.411). Lorentz and polarization corrections were applied. After duplicate and equivalent measurements ($R_{int} = 0.0656$) were averaged and the systematic absences were deleted, 7971 unique observations remained; of these 6600 had $I > 2\sigma(I)$.

The structure was solved by Patterson and Fourier methods and refined using the SHELXL-93 program.[14] All non-hydrogen atoms except those of the solvent were assigned anisotropic displacement parameters. All hydrogen atoms were constrained to idealized geometries and their positions refined riding on their parent carbon atoms with a common thermal isotropic parameter. No restraints were applied. Full-matrix least squares refinement on F^2 of this model (794 parameters) against all data with $I > -3\sigma(I)$ converged to final residual indices given in Table 1. Weights, *w*, were set equal to $[\sigma_c^2(F_o^2) + (gP)^2]^{-1}$, where $P = [\max(F_o^2,0) + 2F_c^2]/3$ and $g = 0.0800$ was chosen to minimize variation of *S* with F_c^2. Final difference electron density maps showed no features outside the range +1.52 to −1.57 e$^-$ Å^{-3}. The largest features were close to the platinum atoms (less than 1 Å). Table 2 lists the final atomic positional parameters for the freely refined atoms. Selected bond lengths and interbond angles are listed in Table 3.

X-ray Structure Analysis of 3. A crystal of **3** (approximate dimensions 0.40 × 0.25 × 0.25 mm) was glued with epoxy adhesive

---

(11) Usón, R.; Forniés, J. *Adv. Organomet. Chem.* **1988**, *28*, 188.

(12) SMART Siemens Molecular Analysis Research Tool V4.014, copyright 1989−94 SAXI.

(13) SAINT (Siemens Area detector INTegration) program V4.021, copyright 1989−94 SAXI.

(14) SHELXTL: Software Package for the Determination of Crystal Structure, Release 5.03; Siemens Analytical X-Ray Instruments Inc., Madison, WI, 1994.

Table 2. Atomic Coordinates ($\times 10^4$) and Equivalent Isotropic Displacement Parameters ($Å^2 \times 10^3$) for $[NBu_4][(C_6F_5)_3Pt(\mu\text{-}Pb)(\mu\text{-}Cl)Pt(C_6F_5)_3]$ (**1**)[a]

	x	*y*	*z*	*U*(eq)		*x*	*y*	*z*	*U*(eq)
Pb	3036(1)	−3307(1)	4347(1)	34(1)	F(21)	3109(2)	−107(4)	2409(4)	67(2)
Pt(1)	3857(1)	−3168(1)	4099(1)	31(1)	F(22)	2818(2)	416(4)	3603(4)	70(2)
Pt(2)	2895(1)	−3019(1)	2971(1)	35(1)	F(23)	2491(2)	−581(4)	4507(3)	58(2)
Cl	3643(1)	−2856(1)	2916(1)	31(1)	F(24)	2490(2)	−2044(3)	4253(3)	44(2)
C(1)	3864(3)	−4317(6)	3943(5)	32(2)	C(25)	2274(3)	−3155(6)	2846(5)	36(3)
C(2)	4116(3)	−4620(7)	3418(6)	44(3)	C(26)	2094(3)	−3052(6)	2192(6)	43(3)
C(3)	4155(4)	−5375(6)	3296(6)	49(3)	C(27)	1676(4)	−3122(7)	2046(7)	56(4)
C(4)	3953(4)	−5878(6)	3689(6)	49(3)	C(28)	1409(4)	−3306(7)	2543(7)	55(3)
C(5)	3713(3)	−5625(6)	4203(6)	45(3)	C(29)	1569(3)	−3407(7)	3204(6)	47(3)
C(6)	3675(3)	−4868(7)	4304(6)	45(3)	C(30)	1999(3)	−3357(6)	3346(6)	42(3)
F(2)	4326(2)	−4130(4)	3038(3)	58(2)	F(26)	2337(2)	−2863(4)	1674(3)	55(2)
F(3)	4395(3)	−5598(4)	2804(4)	78(2)	F(27)	1518(2)	−3025(5)	1380(4)	72(2)
F(4)	3995(2)	−6611(4)	3579(4)	71(2)	F(28)	1000(2)	−3375(5)	2408(4)	85(3)
F(5)	3519(2)	−6123(4)	4595(4)	68(2)	F(29)	1318(2)	−3596(5)	3706(4)	68(2)
F(6)	3428(2)	−4643(4)	4816(3)	53(2)	F(30)	2142(2)	−3482(4)	4012(3)	54(2)
C(7)	3930(3)	−2035(6)	4268(6)	40(3)	C(31)	2982(3)	−4118(6)	2674(5)	38(3)
C(8)	4294(3)	−1702(6)	4083(6)	47(3)	C(32)	3146(3)	−4282(7)	2049(6)	45(3)
C(9)	4388(4)	−946(7)	4198(8)	66(4)	C(33)	3242(4)	−4994(8)	1835(6)	54(3)
C(10)	4099(4)	−498(7)	4506(7)	61(4)	C(34)	3156(4)	−5603(8)	2253(7)	56(4)
C(11)	3731(4)	−811(7)	4707(6)	54(3)	C(35)	2990(3)	−5471(6)	2873(7)	50(3)
C(12)	3659(3)	−1571(6)	4604(5)	37(2)	C(36)	2907(3)	−4753(7)	3073(5)	42(3)
F(8)	4589(2)	−2095(4)	3773(4)	66(2)	F(32)	3229(2)	−3729(4)	1609(3)	62(2)
F(9)	4750(2)	−637(5)	4031(5)	99(3)	F(33)	3394(2)	−5132(5)	1238(4)	82(3)
F(10)	4178(3)	237(4)	4611(5)	89(3)	F(34)	3226(2)	−6311(4)	2062(4)	78(2)
F(11)	3456(2)	−373(4)	5000(4)	70(2)	F(35)	2908(2)	−6048(4)	3290(4)	68(2)
F(12)	3298(2)	−1845(3)	4806(3)	46(2)	F(36)	2743(2)	−4659(4)	3698(3)	51(2)
C(13)	4121(3)	−3345(5)	5060(5)	33(2)	N	918(3)	2995(6)	4273(5)	44(2)
C(14)	4534(3)	−3538(6)	5103(6)	45(3)	C(37)	814(4)	3748(7)	3939(6)	57(3)
C(15)	4772(3)	−3578(7)	5718(6)	45(3)	C(38)	909(4)	3866(8)	3205(7)	68(4)
C(16)	4588(3)	−3429(7)	6317(6)	50(3)	C(39)	846(6)	4682(9)	3000(9)	93(6)
C(17)	4166(3)	−3261(7)	6298(6)	45(3)	C(40)[b]	841(10)	4851(17)	2289(14)	99(10)
C(18)	3945(3)	−3209(6)	5679(5)	34(2)	C(40′)[c]	444(12)	4789(27)	2859(19)	93(15)
F(14)	4737(2)	−3656(4)	4511(3)	52(2)	C(41)	796(4)	3001(6)	5031(5)	44(3)
F(15)	5178(2)	−3759(5)	5717(4)	65(2)	C(42)	351(4)	3149(7)	5145(6)	49(3)
F(16)	4814(2)	−3443(5)	6917(3)	71(2)	C(43)	286(4)	3181(8)	5935(6)	59(3)
F(17)	3989(2)	−3100(4)	6896(3)	63(2)	C(44)	−143(4)	3470(9)	6069(8)	80(5)
F(18)	3534(2)	−3043(4)	5702(3)	47(2)	C(45)	1383(3)	2840(7)	4260(6)	47(3)
C(19)	2816(3)	−1884(6)	3179(6)	40(3)	C(46)	1669(3)	3461(7)	4529(6)	51(3)
C(20)	2965(3)	−1357(6)	2735(5)	41(3)	C(47)	2127(4)	3184(7)	4574(8)	63(4)
C(21)	2967(3)	−592(7)	2878(6)	47(3)	C(48)	2424(4)	3796(9)	4822(8)	88(5)
C(22)	2806(4)	−326(6)	3469(6)	45(3)	C(49)	680(4)	2405(7)	3861(6)	58(3)
C(23)	2648(3)	−827(6)	3924(6)	41(3)	C(50)	712(4)	1608(7)	4122(7)	62(4)
C(24)	2657(3)	−1576(6)	3771(6)	41(3)	C(51)	505(5)	1093(8)	3615(8)	84(5)
F(20)	3115(2)	−1575(4)	2141(3)	55(2)	C(52)	473(6)	317(8)	3813(10)	105(6)

[a] *U*(eq) is defined as one-third of the trace of the orthogonalized U_{ij} tensor. [b] Occupancy 0.6. [c] Occupancy 0.4.

Table 3. Selected Bond Distances (Å) and Angles (deg) for $[NBu_4][(C_6F_5)_3Pt(\mu\text{-}Pb)(\mu\text{-}X)Pt(C_6F_5)_3]$ [X = Cl (**1**), OH (**3**)]

	X = Cl	X = OH		X = Cl	X = OH
Pt(1)−Pb	2.721(1)	2.701(1)	Pt(2)−Pb	2.729(1)	2.712(1)
Pt(1)−C(1)	2.070(10)	2.091(14)	Pt(2)−C(19)	2.082(11)	2.069(13)
Pt(1)−C(7)	2.059(11)	2.074(2)	Pt(2)−C(25)	2.010(10)	1.985(16)
Pt(1)−C(13)	2.024(10)	1.979(16)	Pt(2)−C(31)	2.067(11)	2.069(13)
Pt(1)−X	2.421(2)	2.123(9)	Pt(2)−X	2.431(2)	2.133(9)
Pb···F(6)	2.819(6)	2.962(10)	Pb···F(24)	2.854(6)	3.018(9)
Pb···F(12)	2.867(6)	2.893(9)	Pb···F(30)	2.924(6)	2.925(10)
Pb···F(18)	3.032(6)	2.944(10)	Pb···F(36)	2.851(6)	2.865(8)
Pt(1)−Pb−Pt(2)	85.25(3)	80.5(1)	Pt(1)−X−Pt(2)	99.03(9)	110.4(4)
Pb−Pt(1)−X	87.96(6)	84.8(2)	Pb−Pt(2)−X	87.58(6)	84.4(2)
Pb−Pt(1)−C(1)	87.4(2)	90.6(4)	Pb−Pt(2)−C(31)	94.3(3)	95.7(4)
Pb−Pt(1)−C(7)	99.4(3)	94.6(4)	Pb−Pt(2)−C(19)	91.4(3)	91.4(4)
Pb−Pt(1)−C(13)	100.4(3)	100.7(5)	Pb−Pt(2)−C(25)	101.6(3)	102.7(4)
C(13)−Pt(1)−C(7)	88.3(4)	94.1(6)	C(25)−Pt(2)−C(19)	90.6(4)	87.9(6)
C(13)−Pt(1)−C(1)	88.5(4)	90.3(6)	C(25)−Pt(2)−C(31)	90.1(4)	91.6(5)
C(7)−Pt(1)−C(1)	172.9(4)	172.5(6)	C(19)−Pt(2)−C(31)	174.9(4)	172.8(6)
C(13)−Pt(1)−X	171.0(3)	174.2(5)	C(25)−Pt(2)−X	170.6(3)	172.9(5)
C(1)−Pt(1)−X	95.4(3)	91.6(4)	C(19)−Pt(2)−X	91.4(3)	93.1(5)
C(7)−Pt(1)−X	87.0(3)	83.5(4)	C(31)−Pt(2)−X	87.2(3)	86.5(4)

to the end of a glass fiber. All diffraction measurements were made at room temperature on a Siemens P3m diffractometer, using graphite monochromated Mo Kα *X*-radiation, by using Wyckoff ω scans. Table 1 summarizes the crystallographic data, details associated with data collection, and least squares residuals for the crystal determination of **3**. Unit cell dimensions were determined from 25 centered reflections

Table 4. Atomic Coordinates ($\times 10^4$) and Equivalent Isotropic Displacement Parameters ($Å^2 \times 10^3$) for $[NBu_4][(C_6F_5)_3Pt(\mu\text{-}Pb)(\mu\text{-}OH)Pt(C_6F_5)_3]$ (**3**)[a]

	x	*y*	*z*	*U*(eq)		*x*	*y*	*z*	*U*(eq)
Pb	1399(1)	495(1)	1494(1)	55(1)	C(11)	−2073(16)	2905(12)	1816(11)	66(5)
Pt(1)	1049(1)	1425(1)	2909(1)	50(1)	C(12)	−1277(14)	1606(11)	1720(11)	65(5)
Pt(2)	2897(1)	2113(1)	1630(1)	49(1)	C(13)	−171(14)	497(10)	3159(10)	65(5)
O	2295(8)	2519(6)	2725(5)	61(3)	C(14)	−380(17)	638(12)	3917(11)	68(5)
F(2)	3287(8)	2512(6)	4373(5)	83(3)	C(15)	−1207(17)	89(15)	4189(12)	72(5)
F(3)	5364(9)	2117(6)	5136(5)	96(3)	C(16)	−1873(17)	−720(13)	3660(15)	82(6)
F(4)	5860(9)	470(7)	4662(6)	103(3)	C(17)	−1743(17)	−938(12)	2880(13)	72(5)
F(5)	4160(9)	−835(7)	3474(6)	106(4)	C(18)	−892(17)	−346(11)	2663(11)	67(5)
F(6)	2091(8)	−455(5)	2677(5)	81(3)	C(19)	1372(13)	2463(10)	1003(9)	54(4)
F(8)	299(9)	3232(6)	3581(5)	89(3)	C(20)	1184(13)	3318(10)	1244(9)	58(4)
F(9)	−1275(10)	4130(6)	2945(7)	119(4)	C(21)	258(16)	3628(11)	879(10)	63(5)
F(10)	−2915(10)	3342(7)	1506(7)	115(4)	C(22)	−628(17)	3053(14)	199(12)	85(6)
F(11)	−2882(9)	1671(6)	670(6)	93(3)	C(23)	−490(16)	2228(13)	−59(10)	75(5)
F(12)	−1193(7)	811(6)	1234(5)	79(3)	C(24)	498(14)	1928(10)	332(9)	60(4)
F(14)	285(8)	1429(6)	4477(5)	79(3)	C(25)	3610(13)	1883(10)	653(9)	53(4)
F(15)	−1372(9)	292(6)	4935(6)	90(3)	C(26)	4268(15)	2554(11)	440(11)	65(5)
F(16)	−2732(10)	−1272(7)	3902(7)	109(4)	C(27)	4800(15)	2466(14)	−233(12)	68(5)
F(17)	−2378(9)	−1706(6)	2390(7)	111(4)	C(28)	4684(17)	1598(16)	−729(10)	76(6)
F(18)	−777(9)	−598(6)	1893(6)	85(3)	C(29)	4067(16)	895(12)	−525(11)	67(5)
F(20)	1969(8)	3925(5)	1902(5)	83(3)	C(30)	3528(16)	1030(12)	135(10)	62(5)
F(21)	97(9)	4473(7)	1137(6)	108(4)	C(31)	4546(12)	1929(10)	2286(7)	44(4)
F(22)	−1588(10)	3344(7)	−169(6)	113(4)	C(32)	5405(15)	2659(11)	2919(10)	64(4)
F(23)	−1304(9)	1652(7)	−719(6)	108(4)	C(33)	6409(15)	2590(12)	3366(8)	59(4)
F(24)	547(7)	1062(5)	37(5)	68(3)	C(34)	6733(17)	1815(13)	3339(10)	70(5)
F(26)	4357(8)	3414(6)	899(5)	78(3)	C(35)	5917(15)	1037(12)	2794(10)	65(5)
F(27)	5419(10)	3186(7)	−394(6)	101(3)	C(36)	4859(14)	1140(10)	2306(8)	49(4)
F(28)	5227(10)	1544(7)	−1356(6)	102(3)	N	5431(13)	6055(9)	2817(8)	81(4)
F(29)	3979(9)	97(7)	−1002(5)	95(3)	C(37)	4663(16)	6734(12)	2689(10)	92(6)
F(30)	2950(8)	289(6)	274(5)	71(3)	C(38)	3301(19)	6402(14)	2181(13)	130(8)
F(32)	5168(8)	3488(6)	2865(6)	94(3)	C(39)	2561(23)	7109(17)	2225(15)	144(9)
F(33)	7180(9)	3349(7)	3880(6)	104(4)	C(40)[b]	1082(24)	6790(27)	2049(26)	125(15)
F(34)	7731(9)	1754(7)	3856(6)	100(3)	C(40′)[c]	1857(44)	7125(32)	2908(22)	152(19)
F(35)	6173(8)	239(6)	2800(5)	84(3)	C(41)	5700(16)	5538(12)	2042(10)	87(6)
F(36)	4043(8)	353(5)	1849(5)	68(2)	C(42)	6565(18)	6005(13)	1647(11)	102(6)
C(1)	2620(13)	1056(10)	3496(8)	48(4)	C(43)	6805(22)	5434(15)	910(13)	146(9)
C(2)	3491(14)	1681(12)	4120(9)	60(4)	C(44)	7715(22)	5852(16)	526(14)	169(10)
C(3)	4558(15)	1483(13)	4518(9)	64(5)	C(45)	6685(17)	6554(12)	3400(11)	93(6)
C(4)	4783(16)	631(14)	4291(11)	72(5)	C(46)	7685(18)	6041(13)	3596(12)	117(7)
C(5)	3926(17)	−28(11)	3674(10)	66(5)	C(47)	8896(23)	6641(16)	4133(15)	160(10)
C(6)	2875(16)	202(10)	3303(9)	62(5)	C(48)	9950(26)	6291(20)	4339(18)	252(17)
C(7)	−406(13)	1959(10)	2422(9)	51(4)	C(49)	4703(18)	5376(13)	3145(11)	101(6)
C(8)	−505(15)	2796(11)	2843(10)	65(5)	C(50)	4160(19)	5665(14)	3856(12)	117(7)
C(9)	−1263(18)	3291(12)	2546(11)	78(6)	C(51)	3318(27)	4871(19)	4018(17)	191(12)
C(10)	−2103(15)	2057(12)	1384(11)	71(5)	C(52)	2789(30)	5042(21)	4588(18)	277(20)

[a] *U*(eq) is defined as one-third of the trace of the orthogonalized U_{ij} tensor. [b] Occupancy 0.5. [c] Occupancy 0.5.

in the range $14.7 < 2\theta < 28.5°$. A total of 10 748 reflection intensities was measured in an unique hemisphere of reciprocal space for $3.0 < 2\theta < 50.0°$ by Wyckoff ω scans. Three check reflections remeasured after every 150 ordinary data showed no decay and variation of ±3% over the period of data collection. An absorption correction was applied on the basis of 864 azimuthal scan data (maximum and minimum transmission coefficients were 1.000 and 0.561). Lorentz and polarization corrections were applied. After duplicate and equivalent measurements ($R_{int} = 0.065$) were averaged and systematic absences were deleted, 9950 unique observations remained; of these 5138 had $I > 2\sigma(I)$.

The structure was solved by Patterson and Fourier methods and refined using SHELXL-93. All non-hydrogen atoms except the carbon atoms of NBu_4^+ were assigned anisotropic displacement parameters. All hydrogen atoms were constrained to idealized geometries and their positions refined riding on their parent carbon atoms with a common thermal isotropic parameter. One methyl group of NBu_4^+ is disordered over two positions (partial occupancy 0.5), and the C−C distances of both sets were constrained to 1.54 Å. Full-matrix least squares refinement on F^2 of this model (709 parameters) against all data with $I > -3\sigma(I)$ converged to final residual indices given in Table 1. Weights, *w*, were set equal to $[\sigma_c^2(F_o^2) + (gP)^2]^{-1}$, where $P = [\max(F_o^2,0) + 2F_c^2]/3$ and $g = 0.0500$ was chosen to minimize variation of *S* with F_c^2. Final difference electron density maps showed no features outside the range +0.82 to −0.74 e $Å^{-3}$. Table 4 lists the final atomic positional parameters for the freely refined atoms. The largest features were close to the disordered methyl group of NBu_4^+. Selected bond lengths and interbond angles are listed in Table 3.

UV/vis Spectra. The UV/vis absorption spectra were recorded at 300 K on a Hitachi U-3400 spectrophotometer. Photoluminescence spectra were obtained by exciting the samples with light from a 1000 W tungsten lamp passed through a 0.5 m double monochromator. Fluorescence was detected through a 0.5 m monochromator with photomultiplier detector. The luminescence spectra were corrected for instrumental response using a standard tungsten−halogen lamp calibrated against a National Institute of Standards and Technology.

Results and Discussion

The reaction between $[NBu_4]_2[Pt(C_6F_5)_3X]$ (X = Cl, I) and $Pb(ClO_4)_2 \cdot 3H_2O$ in CH_2Cl_2 provides $[NBu_4][(C_6F_5)_3Pt(\mu\text{-}Pb)(\mu\text{-}X)Pt(C_6F_5)_3]$ (X = Cl (**1**), I (**2**)) in good yield (70% in both complexes, eq 1). Although the stoichiometry requires a 3:4

$$4[NBu_4]_2[Pt(C_6F_5)_3X] + 3Pb(ClO_4)_2 \xrightarrow{CH_2Cl_2}$$

$$2[NBu_4][(C_6F_5)_3Pt(\mu\text{-}Pb)(\mu\text{-}X)Pt(C_6F_5)_3] +$$

$$X = Cl\ (\mathbf{1}), I\ (\mathbf{2})$$

$$6NBu_4ClO_4 + PbX_2 \quad (1)$$

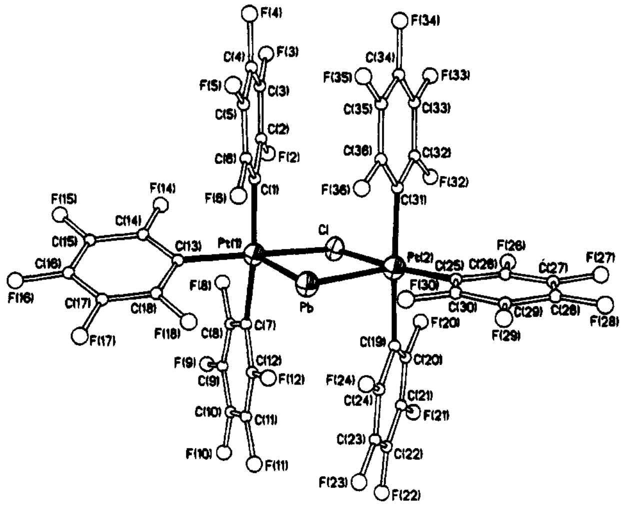

Figure 1. Molecular structure of the anion of **1** showing the full atom labeling scheme. Metal and chlorine atoms are drawn to enclose 50% probability density.

(Pb:Pt) molar ratio (eq 1), we have observed that a better yield can be obtained if the reaction is carried out with a 1:1 molar ratio. The excess of the insoluble $Pb(ClO_4)_2$ and the PbX_2, formed in the reaction, are easily eliminated from the reaction mixture by filtration.

Complexes **1** and **2** are air stable in the solid state and in anhydrous solvents. In solution, the presence of moisture leads to the hydrolysis of the Pt−X bonds. Thus, complex **1** in CH_2Cl_2 reacts with H_2O to form $[NBu_4][(C_6F_5)_3Pt(\mu\text{-}Pb)(\mu\text{-}OH)Pt(C_6F_5)_3]$ (**3**) in a slow reaction which requires several hours to go to completion (eq 2).

$$[NBu_4][(C_6F_5)_3Pt(\mu\text{-}Pb)(\mu\text{-}Cl)Pt(C_6F_5)_3] + H_2O \xrightarrow{CH_2Cl_2} [NBu_4][(C_6F_5)_3Pt(\mu\text{-}Pb)(\mu\text{-}OH)Pt(C_6F_5)_3] + HCl \quad (2)$$

Complex **3** can also be prepared, although in a slightly lower yield, by reacting $[NBu_4]_2[Pt(C_6F_5)_3Cl]$ with $[NBu_4]OH$ and $Pb(ClO_4)_2$.

Structures of 1 and 3. The structures of **1** and **3** have been established by X-ray diffraction methods and are very similar. Due to the similarity of both anions, only the structure of the anion of **1** is shown in Figure 1. Table 3 lists selected bond distances and bond angles for both anions, for which the same atom numbering scheme has been used. We give here a complete description of only the anion of **1** (the analogous distances and angles for **3** are presented in brackets), and then we will comment on the principal differences between the two anions.

The anions formally result from the interaction of dinuclear $[(C_6F_5)_3Pt(\mu\text{-}X)Pt(C_6F_5)_3]^{3-}$ with Pb^{2+}, the former acting as a didentate cheating ligand by means of two Pt → Pb donor−acceptor bonds, unsupported by a covalent bridging ligand. The Pt−Pb distances Pt(1)−Pb = 2.721(1) Å [2.701(1) Å], Pt(2)−Pb = 2.729(1) Å [2.712(1) Å] are slightly shorter than the ones found in linear $[(C_6F_5)_4Pt-Pb-Pt(C_6F_5)_4]^-$ {2.769(2) Å, 2.793(2) Å}.[3]

Each platinum center is in a distorted square pyramidal environment formed by three C_6F_5 groups and one $\mu\text{-}X^-$ ligand (X = Cl (**1**), OH (**3**)), which constitute the base of the pyramid, with Pb^{2+} in the apical site. The Pt−Pb bonds are almost perpendicular to the basal planes, the angles between these bonds and the perpendicular to the their respective planes being 6.6(2)° [6.6(3)°] for Pt(1)−Pb and 3.7(2)° [7.7(3)°] for Pt(2)−Pb. The platinum atoms are slightly displaced from the basal (C_3X) plane toward the Pb atom by 0.11 Å [0.10 Å] for Pt(1) and 0.11Å [0.13 Å] for Pt(2). The Pt−C distances are similar to Pt−C distances found in other complexes containing the $Pt(C_6F_5)_3X$ fragment.[15−17]

The Pt−X bridge distances (X = Cl, 2.421(2) and 2.431(2) Å [X = OH, 2.123(9) and 2.133(9) Å]) and the Pt−X−Pt angles (99.03(9)° [110.4(4)°] in complexes **1** and **3** are similar to those found in other (μ-chloro)- or (μ-hydroxo)platinum(II)[2,18−21] or -palladium(II)[22−24] complexes. The distances between the oxygen atom and some of the *o*-fluorine atoms (around 3 Å) could indicate the existence of some hydrogen bonding.

Finally, the lead atom, which is essentially two-coordinated, is bonded to two platinum centers in an angular way {Pt(1)−Pb−Pt(2) = 85.3(1)° [80.4(1)°]} and displays three pairs of short *o*-F···Pb contacts of different strength {2.819(6)−3.032(6) Å}, similar to F···M interactions observed in related Pt → M complexes containing C_6F_5 ligands.[1]

The two-coordinate environment of Pb^{2+} is remarkable, since in other polynuclear M−Pb(II) complexes, which contain two M−Pb(II) single bonds, Pb(II) typically displays a higher coordination number $[Pb\{Mo(\eta\text{-}C_5Me_5)(CO)_3\}_2(OC_4H_8)]$,[25] $[\{Pb[Mo(\eta\text{-}C_5Me_5)(CO)_3][Mo(\eta\text{-}C_5Me_5)(CO)_2(\mu\text{-}CO)]\}_2]$,[25] $[Ir_2(PbI)(CO)_2I_2(\mu\text{-}dpma)_2]$ and $[Ir(PbNO_3)(CO)_2X_2(\mu\text{-}dpma)_2][NO_3]$ (X = Cl, Br, I; dpma = bis((diphenylphosphino)methyl)phenylarsine),[6] and $[Au_2Pb(MTP)_4]$ [MTP = $CH_2P(S)Ph_2^-$].[5] The low coordination number for Pb in **1** and **3** could well be due to the presence of the six *o*-F···Pb nonbonding contacts which stabilize the polynuclear compound and complete the coordination requirements of the Pb(II) center. Notably, in the other structurally characterized pentafluorophenyl Pt−Pb(II) compounds $[NBu_4]_2[(C_6F_5)_4Pt-Pb-Pt(C_6F_5)_4]$,[3] the Pb(II) center is also two-coordinated and shows eight *o*-F···Pb(II) contacts.

Comparing the anions of complexes **1** and **3**, it can be seen that the Pt−Pb distances are rather similar in both cases (perhaps suggesting similar basicity of the two $[(C_6F_5)_3Pt(\mu\text{-}X)Pt(C_6F_5)_3]^-$ units) and that the most important structural difference between the two anions is related to the different size of the X atom (X = Cl (**1**), O (**3**)) which bridges the platinum centers. This results in longer Pt−Cl than Pt−O distances, and perceptible differences are also observed on the Pt(1)···Pt(2) distances [3.691(1) Å (**1**), 3.495(1) Å (**3**)] and on the Pt−X−Pt, Pt−Pb−Pt and X−Pt−Pb angles (see Table 3).

NMR Spectra. The ^{19}F NMR spectra of complexes **1**−**3** are very similar. The ^{19}F NMR spectrum of $[NBu_4][(C_6F_5)_3Pt(\mu\text{-}Pb)(\mu\text{-}Cl)Pt(C_6F_5)_3]$ (**1**) in $CDCl_3$ at room temperature, which is presented in Figure 2, shows four multiplets on the

---

(15) Usón, R.; Forniés, J.; Tomás, M.; Ara, I. *J. Chem. Soc., Dalton Trans.* **1989**, 1011.
(16) Usón, R.; Forniés, J.; Tomás, M.; Ara, I. *J. Chem. Soc., Dalton Trans.* **1990**, 3151.
(17) Cotton, F. A.; Falvello, L. R.; Usón, R.; Forniés, J.; Tomás, M.; Casas, J. M.; Ara, I. *Inorg. Chem.* **1987**, *26*, 1366.
(18) Rochon, F. D.; Morneau, A.; Melanson, R. *Inorg. Chem.* **1988**, *27*, 10.
(19) Alcock, N. W.; Bergamini, P.; Gomes-Carneiro, T. M.; Nicholls, J.; Orpen, A. G.; Pringle, P. G.; Sostero, S.; Traverso, O. *J. Chem. Soc., Chem. Commun.* **1990**, 980.
(20) Trovo, C.; Bandolini, G.; Casellato, U.; Corani, B.; Nicolini, M.; Longato, B. *Inorg. Chem.* **1990**, *29*, 4616.
(21) Usón, R.; Forniés, J.; Tomás, M., Usón, I. *Angew. Chem., Int. Ed. Engl.* **1990**, *29*, 1449.
(22) Forniés, J.; Navarro, R.; Sicilia, V.; Martinez, F.; Welch, A. J. *J. Organomet. Chem.* **1991**, *408*, 425.
(23) Grove, D. M.; van Koten, G.; Ubbels, H. J. C.; Spek, A. L. *J. Am. Chem. Soc.* **1982**, *104*, 4285.
(24) Braunstein, P.; Luke, M. A. *New J. Chem.* **1988**, *12*, 429.
(25) Hitchcock, P. B.; Lappert, M. F.; Michalczyk, M. J. *J. Chem. Soc., Dalton Trans.* **1987**, 2635.

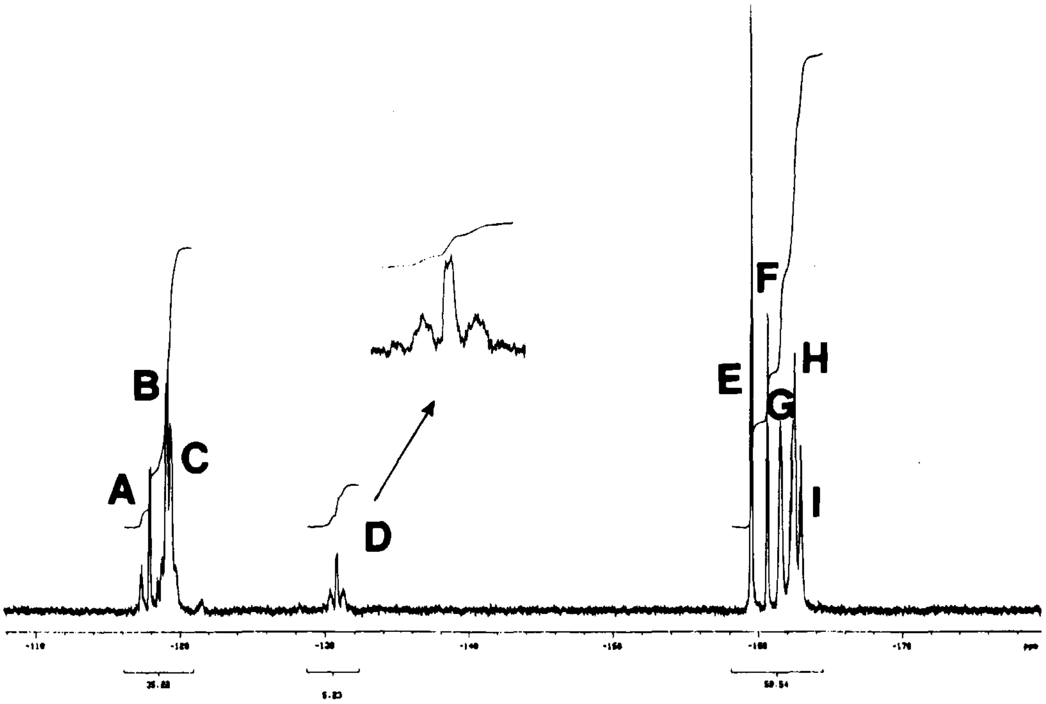

Figure 2. ^{19}F NMR spectrum of complex **1**.

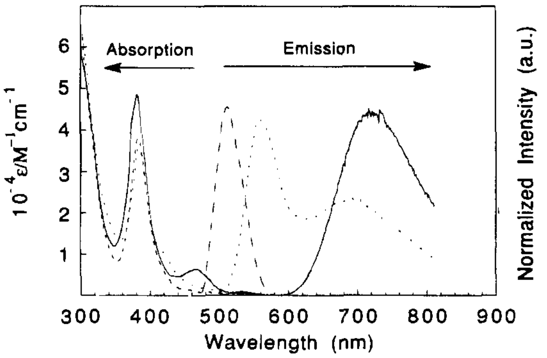

Figure 3. 300 K absorption and emission spectra of (dashed line) complex **1**, (dotted line) complex **2**, and (solid line) complex **3**.

o-fluorine region: two of them, signals B and C at −119.1 and −119.4 ppm, are due to four *o*-fluorine atoms which correspond to the C_6F_5 groups in the *trans* position; the other two (A and D at −130.8 and −117.9 ppm) can be assigned to the *o*-F atoms of the pentafluorophenyl rings *trans* to the chloride. The differences between these two signals are noteworthy; D is shifted to lower frequencies, and the intensity of its satellites indicates that this fluorine atom is coupled to both platinum and lead nuclei. Moreover, the ^{19}F NMR spectrum shows two triplets due to the *p*-F atoms at −159.5 (4F) and −160.6 (2F) ppm (signals E and F) and four multiplets [−161.5 (4F), −162.3 (2F), −162.5 (4F), and −162.9 (2F) ppm] (signals G, H, I, and F) which correspond to the *m*-fluorine atoms.

Optical Properties. Since the Pt−Pb bonds involved in these complexes are the result of the interaction between d^8 and s^2 centers and, usually, polynuclear complexes with this type of interaction are luminescent,[6] a spectroscopic study has been carried out on complexes **1**−**3**. The optical absortion spectra of the three compounds, both in the solid state and in CCl_4 solutions, have been measured at 300 K. The solution spectra are plotted in Figure 3. Intense absortions bands at *ca.* 290 nm (not shown in Figure 3) and 380 nm can be seen for the three compounds (ϵ (380 nm band) $\approx 3.3 \times 10^4$ M^{-1} cm^{-1} for complexes **1** and **2**; $\epsilon \approx 4 \times 10^4$ M^{-1} cm^{-1} for complex **3**). These bands are similar to those found for $[Ir_2M(CO)_2X_2(\mu\text{-dpma})_2]^+$ (M = Tl, SbF_2, $PbNO_3$ and X = Cl; M = PbI and X = I)[6] and $[Au_2Pb(MTP)_4]$[5] and may be due to transitions between filled and empty molecular orbitals of the Pt−Pb−Pt units in **1**−**3**.[5,6]

Besides these absorption bands, a much less intense band ($\epsilon \approx 0.5 \times 10^4$ M^{-1} cm^{-1}) appears at *ca.* 470 nm in the spectrum of complex **3**. A shoulder at *ca.* 415 nm can be observed in the spectrum of complex **2**. The Pt−X distances strongly depend on the ligand X; thus we tentatively assign these low-energy absorptions to transitions from the ground state to metal-to-ligand charge transfer states (mlct) lying below the metal−metal first excited state.

The absorption spectra of solid samples qualitatively coincide with those of solutions. The solid of complex **3** shows an intense red emission at 720 nm (half-width *ca.* 2900 cm^{-1}), whereas complex **1** only presents a faint yellow-green emission at about 510 nm (half-width 1770 cm^{-1}). As can be seen in Figure 3, the emission spectrum of complex **2** is an intermediate case between these two. The excitation spectra roughly coincide with the absorption ones. Presumably the emission arises from the mlct relaxed state. It is interesting to notice that the strongest emission efficiency corresponds to the strongest mlct absorption. This may indicate that there is a competition between nonradiative multiphonon and radiative emissions the latter being stronger for the complex with larger radiative ground state mlct transition probability.

Acknowledgment. We are grateful to the Dirección General de Investigación Científica y Técnica (DGICYT) for financial support (Project PB92-0364) and for a grant to A.M. and A.J.R.

Supporting Information Available: A drawing of the structure of the anion of **3** showing full atom labeling scheme. For the crystal structures of **1** and **3**, complete tables of bond distances and angles, anisotropic thermal parameters for the non-hydrogen atoms, and hydrogen atom positions and isotropic thermal parameters, and a figure showing the full atom labeling scheme for the structure of the anion of **3** (14 pages). Ordering information is given on any current masthead page.

IC950847+